JOURNAL OF COMPUTATIONAL PHYSICS 6, 183–199 (1970)

A Numerical Model for Viscous, Nondivergent, Barotropic, Wind-Driven, Ocean Circulations

W. P. CROWLEY

Lawrence Radiation Laboratory, University of California, Livermore, California 94550

Received November 21, 1969; revised February 20, 1970

A modified-rigid-lid numerical ocean model consisting of a tendency equation for vorticity and a Helmholtz equation that relates vorticity to a streamfunction is presented. Integration of the vorticity equation involves a fourth-order fractional-time-step method. The Helmholtz equation is inverted by a partial Fourier transform technique. The large scales in the numerical solutions obtained from this model can be made to agree with those obtained from a free-surface model by adjusting the parameter in the Helmholtz equation. A comparison of computational speeds made between this model and a free-surface model shows the modified-rigid-lid model to be faster by a factor of five.

I. INTRODUCTION

In a previous article [1] a numerical model for viscous, free-surface barotropic flow in a wind-driven ocean basin was presented. It was pointed out that if gravity waves could be excluded from the model, the integration time step could be increased by more than an order of magnitude. We shall continue this investigation here by considering a numerical model from which these waves have been excluded. We will consider only the transient solution in the barotropic case with the hope that the techniques developed can later be applied to baroclinic models (where integration times of the order of centuries [2] may be necessary). Although both internal and external gravity waves may exist in baroclinic models, we consider here only the barotropic case so that statements about gravity waves pertain only to external gravity waves. We will find that although the rigid-lid filter seriously distorts the transient solution, the filter can be modified so that reasonable large scale approximations to the free-surface transient solution may be obtained with filtered equations.

It is usually assumed that gravity waves contribute very little information to the solution of large scale ocean circulation problems; in excluding these waves from the solution, the exclusion process itself may, however, exert a considerable effect on the solution. The filtering is usually accomplished by adjusting the

equations of motion so that physical phenomena responsible for these waves are inoperative. For example, according to Thompson [3], Charney found that solutions from geostrophic models are free from gravity waves. Moreover, Charney's geostrophic filter approximately preserves the phase speed of Rossby waves. We choose to follow a different course from Charney's; recognizing that gravity waves are vertical-transverse waves, we see that the elimination of a free upper surface precludes the existence of these waves. After Bryan [4] we shall then in effect clamp a rigid lid onto the basin; the resulting rigid-lid equations consist of a tendency equation for vorticity and a Poisson equation relating the streamfunction to the vorticity.

An alternate, quite interesting, rigid-lid method employed by Berdahl [5] does not explicitely make use of a streamfunction—rather the incompressibility condition is used to relate the pressure to the velocity field through an elliptic equation. The pressure then provides an acceleration for the primitive equations.

Unfortunately, the rigid-lid equations drastically increase the phase speed of Rossby waves; a rigid-lid model will thus fail in simulating the transient response of an ocean basin. However, if we modify the rigid-lid equations by replacing the Poisson equation with a Helmholtz equation, we somewhat heuristically introduce a parameter that may be adjusted to slow down the Rossby waves. The model presented here thus consists of modified-rigid-lid equations and it can be shown that for the scales of motion considered, the modified-rigid-lid equations are approximately equivalent to Charney's geostrophically filtered equations.

The equations of the model are solved by finite difference techniques. A fourth-order time-splitting technique is used for the vorticity tendency equation, and a partial Fourier transform technique is used to invert the Helmholtz equation. It is found that a time step of 2 hr is permitted with a spatial increment of 170 km (this should be compared to a time step of 0.125 hours for the free-surface case).

In the free-surface solution small scale ($\lambda = 2\Delta x$) motions appeared even though the energy source was large scale ($\lambda \sim$ basin size). This then necessitated the inclusion of a horizontal eddy-viscosity for numerical reasons and it was asserted that the small scales were produced from large scales by a cascade of vorticity. It now appears that this assertion was wrong, for in the rigid-lid model it is possible to compute with no explicit eddy diffusion coefficient; at least this is possible for the times of interest in this problem. Further comments on this matter will be found in Section IV.

In Section II, the modified-rigid-lid equations and boundary conditions are presented, a justification for the modification is made, and the equivalence between these equations and the geostrophically filtered equations is noted. Section III contains the finite difference equations and a description of the ocean basin. A comparison of this model with a free-surface model with respect to solutions

and computational speeds is made in Section IV, and a summary of this work appears in Section V.

II. Equations and Boundary Conditions

In this section we will present the equations of motion and the boundary conditions for the modified-rigid-lid model. An *a priori* justification for the modification is made based on linear theory—an *a posteriori* justification will be found in Section IV. However, it must be emphasized that only the early part of the transient barotropic solution is under consideration here. The effect of the Helmholtz term on the steady solution in the barotropic case remains to be studied.

The rigid-lid equations of motion are obtained from those for free-surface flow [1] by imposing the condition $H = \text{constant}$—that is, $\partial h/\partial t = 0$. The continuity equation then admits a streamfunction

$$u = -\frac{\partial \psi}{\partial y}$$

and (II-1)

$$v = \frac{\partial \psi}{\partial x},$$

and cross-differentiation of the two momentum equations transforms them into a vorticity equation,

$$\frac{\partial \zeta}{\partial t} + \frac{\partial \zeta u}{\partial x} + \frac{\partial \zeta v}{\partial y} = -\beta v + \kappa \nabla^2 \zeta + \frac{1}{H}\frac{\partial \tau^x}{\partial y}, \tag{II-2}$$

where

$$\zeta = \frac{\partial v}{\partial x} - \frac{\partial u}{\partial y} \tag{II-3}$$

is the relative vorticity. Equations (II-1) and (II-3) may be combined to give

$$\nabla^2 \psi = \zeta, \tag{II-4}$$

a linear equation relating the streamfunction to the vorticity.

The absolute vorticity $\Lambda = \zeta + f$ obeys the equation

$$\frac{\partial \Lambda}{\partial t} + \frac{\partial \Lambda u}{\partial x} + \frac{\partial \Lambda v}{\partial y} = \kappa \nabla^2 \zeta + \frac{1}{H}\frac{\partial \tau^x}{\partial y}, \tag{II-5}$$

where $f = f_0 + \beta y$ is the Coriolis parameter; $\beta = 0.64 \times 10^{-4}\ \text{km}^{-1}\ \text{hr}^{-1}$. In the absence of wind stress and dissipation, Eq. (II-5) indicates that the total absolute vorticity is a constant of the motion.

Equations (II-2) and (II-4) are the fundamental equations for barotropic nondivergent, wind-driven, viscous flow on a β-plane. (In being consistent with the previous article, we have used the β-plane approximation and have assumed a zonal wind stress and zero bottom drag.)

It is known [6, 7] that Eqs. (II-2) and (II-4) produce solutions in which the phase velocities are too large when compared with free-surface solutions. This is seen for the linear plane wave case, if we assume a solution of the form

$$\psi(x, y, t) = \epsilon^{i(kx+ly-\sigma t)}.$$

Substitution into Eqs. (II-2) and (II-4) gives, if we neglect advection, dissipation and the wind-stress,

$$\sigma = \frac{-k\beta}{k^2 + l^2}$$

while for the free-surface case [8],

$$\sigma = \frac{-k\beta}{k^2 + l^2 + f^2/gH}.$$

The phase speed (σ/k) is thus greater in the nondivergent than in the free-surface case. However, if we replace the Poisson equation (II-4) with a Helmholtz equation

$$(\nabla^2 - \gamma^2)\psi = \zeta, \tag{II-6}$$

where γ^2 is a constant, we find the following relation for the frequency:

$$\sigma = \frac{-k\beta}{k^2 + l^2 + \gamma^2}. \tag{II-7}$$

Comparing this with σ for the free-surface case we have

$$\gamma^2 = f^2/gH. \tag{II-8}$$

Thus we can perhaps slow down the evolution of the nondivergent solution if we use Eq. (II-6) in place of (II-4). The only free parameter is γ, and we will be able to determine it experimentally. In Section IV we will find that the choice

$$gH\gamma^2 = (f_0 + \beta Y/2)^2$$

produces a solution that is quite similar to the free-surface solution.

The differential equations for this model are thus Eqs. (II-2) and (II-6).

Another way of filtering gravity waves from the solution is to make the geostro-

phic approximation (see Thompson [3] p. 79). This approximation leads to a more complicated set of equations than those used here, but the phase of the solution is approximately that of the free-surface case. It can be shown that the geostrophic filtering approximation is equivalent to the rigid-lid filter used here if $\nabla^2\psi \ll f$. It will be seen in the solutions presented here that $\nabla^2\psi \sim 0.003f$, a good indication that for the scales of motion appearing in these solutions, the modified rigid-lid equations (II-2 and II-6) are equivalent to the geostrophically filtered equations.

The boundary conditions used here are identical to those for the free-surface model. We wish to compute the flow in a square basin on a β-plane and we take northern and southern boundaries to be no-transport, free-slip boundaries while along the eastern and western boundaries the no-slip condition is imposed. If $0 \leqslant x \leqslant X$ and $0 \leqslant y \leqslant Y$, we have, for the streamfunction,

$$\psi(x, 0, t) = \psi(x, Y, t) = \psi(0, y, t) = \psi(X, y, t) = 0$$

and for the vorticity,

$$\zeta(x, 0, t) = \zeta(x, Y, t) = 0.$$

Along eastern and western boundaries, the vorticity is permitted to change in time in accordance with Eq. (II-2).

The wind stress is taken to be a function of y alone,

$$\tau^x = K_D \cos \pi y/Y \tag{II-9}$$

and it is seen that the curl of the wind stress does not change sign within the basin.

III. Finite Difference Equations

As in the free-surface model, we employ finite difference techniques here to solve the equations of motion. A square basin 4440 km on a side is subdivided into 26 zones each of which is thus approximately 170 km square. If the space–time mesh-point coordinates are given by $x_k = k\,\Delta x$, $y_l = l\,\Delta y$ and $t_n = n\,\Delta t$ and the primary variables are centered at mesh points, we have $\zeta^n_{k,l}$ and $\psi^n_{k,l}$. The velocities, $u^n_{k,l-1/2}$, $v^n_{k-1/2,l}$ are offset in accordance with Eqs. (II-1).

Given the spatial distribution of vorticity at any time t, the dependent variables are advanced to time $t + \Delta t$ as follows. Equation (II-6) is solved for the streamfunction at time t,

$$\psi^n_{k,l} = (\nabla^2 - \gamma^2)^{-1}\, \zeta^n_{k,l}\,; \tag{III-1}$$

velocities are obtained from the streamfunction,

$$u^n_{k,l-1/2} = \frac{\psi^n_{k,l-1} - \psi^n_{k,l}}{\Delta x}, \qquad v^n_{k-1/2,l} = \frac{\psi^n_{k,l} - \psi^n_{k-1,l}}{\Delta y};$$

and the vorticity is then advanced to $t + \Delta t$ by a finite difference approximation to Eq. (II-2). The details of these calculations follow.

Equation (III-1) is solved by a method used in plasma calculations [9] and related to a method used in a previous ocean circulation calculation [10]. We note that the northern and southern boundary conditions on ζ and ψ permit them to be expanded in a sine series

$$\psi_{k,l} = \sum_{p=1}^{P} a_{k,p} \sin p\pi l \Delta y / Y \tag{III-2}$$

and

$$b_{k,p} = \frac{1}{P+1} \sum_{l=1}^{P} \zeta_{k,l} \sin p\pi l \Delta y / Y, \tag{III-3}$$

where $0 \leqslant l \leqslant P + 1$. If we, for the moment, think of ψ and ζ as continuous variables we may differentiate Eq. (III-2) and substitute into Eq. (II-6) to obtain

$$\frac{d^2}{dx^2} a(x,p) - \left[\left(\frac{p\pi}{Y}\right)^2 + \gamma^2\right] a(x,p) = b(x,p)$$

a set of P ordinary differential equations which are solved by the backward substitution method [11, 12]. A difference equation for a_k is (for fixed p)

$$-a_{k+1} + Qa_k - a_{k-1} = -b_k \Delta x^2, \tag{III-4}$$

where

$$Q(p) = 2 + \left(\frac{p\pi \Delta x}{Y}\right)^2 + \gamma^2 \Delta x^2.$$

Following Richtmyer [12] we assume a relation

$$a_k = E_k a_{k+1} + F_k \tag{III-5}$$

and find

$$E_k = \frac{1}{Q - E_{k-1}}$$

and (III-6)

$$F_k = (F_{k-1} - b_k \Delta x^2) E_k .$$

The boundary conditions on ψ give $E_0 = F_0 = 0$ as starting conditions. Equations (III-6) are solved forward through the mesh for E_k and F_k ; Eq. (III-5) is then solved backwards through the mesh for a_k .

The solution of Eq. (III-1) proceeds as follows. We have ζ and solve Eq. (III-3) for $b_{k,p}$; next Eq. (III-4) is solved for $a_{k,p}$; finally $\psi_{k,l}$ is obtained from Eq. (III-2).

If the eastern and western boundary conditions were changed to free-slip conditions, ζ and ψ could then be expanded in a double Fourier series. This would reduce the set of ordinary differential equations to a set of algebraic equations

$$a_{q,p} = -\frac{b_{q,p}}{\left(\frac{q\pi}{X}\right)^2 + \left(\frac{p\pi}{Y}\right)^2 + \gamma^2},$$

which would produce a more accurate solution to the differential equation. However, this technique would be slower than the partial technique used here by a factor of approximately $X/\Delta x$.

Obviously, Fourier transform techniques depend upon the boundary conditions, and the technique used here is probably not applicable to more realistic ocean basins. In that case, one can resort to iterative techniques to invert the Helmholtz equation (Eq. II-6). According to Ellsaesser [13] the Helmholtz term acts to speed up convergence of these iterative schemes.

Before writing the difference equation for vorticity, we rewrite Eq. (II-2) in a divergence form to display its conservative nature

$$\frac{\partial}{\partial t} = -\frac{\partial F}{\partial x} - \frac{\partial G}{\partial y},$$

where

$$F = \zeta u - \kappa \frac{\partial \zeta}{\partial x} + \beta\psi$$

and

$$G = \zeta v - \kappa \frac{\partial \zeta}{\partial y} - \frac{\tau^x}{H}$$

and note that the total relative vorticity is changed only by boundary fluxes and the wind stress

$$\frac{\partial}{\partial t}\int\int \zeta \, dx \, dy = -2K_D \frac{X}{H} + \kappa \int_0^Y \left[\frac{\partial \zeta}{\partial x}\Big|_X - \frac{\partial \zeta}{\partial x}\Big|_0\right] dy.$$

The advective part of the fluxes F is approximated to fourth order [14] by

$$\frac{\Delta t}{\Delta x}\zeta u\Big|_{k+1/2,l} = \frac{\alpha}{16}[9(\zeta_{k+1,l}+\zeta_{k,l})-(\zeta_{k+2,l}+\zeta_{k-1,l})]$$
$$-\frac{\alpha^2}{48}[27(\zeta_{k+1,l}-\zeta_{k,l})-(\zeta_{k+2,l}-\zeta_{k-1,l})]$$
$$-\frac{\alpha^3}{12}[(\zeta_{k+1,l}+\zeta_{k,l})-(\zeta_{k+2,l}+\zeta_{k-1,l})]$$
$$+\frac{\alpha^4}{24}[3(\zeta_{k+1,l}-\zeta_{k,l})-(\zeta_{k+2,l}-\zeta_{k-1,l})]$$

and a similar form is used for the advective part of G. For points adjacent to boundary points, the above form may not be used, and a second order approximation is necessary [14]; thus for $k = K-1$ or $k = 0$,

$$\frac{\Delta t}{\Delta x}\zeta u\Big|_{k+1/2,l} = \frac{\alpha}{2}(\zeta_{k+1,l}+\zeta_{k,l})-\frac{\alpha^2}{2}(\zeta_{k+1,l}-\zeta_{k,l}).$$

As before, a similar form is used for $l = L-1$ and $l = 0$. In these expressions, the nondimensional parameter α is $u_{k+1/2,l}\,\Delta t/\Delta x$ in the ζu expression and $v_{k,l+1/2}\,\Delta t/\Delta y$ in the ζv expression.

The diffusive flux is given by a centered difference

$$\kappa\frac{\partial\zeta}{\partial x}\Big|_{k+1/2,l} = \frac{\kappa}{\Delta x}(\zeta_{k+1,l}-\zeta_{k,l})$$

and the β-term by an average

$$\beta\psi\,|_{k+1/2,l} = \tfrac{1}{2}\beta(\psi_{k+1,l}+\psi_{k,l}).$$

Once the fluxes F and G have been computed, the vorticity is advanced from t to $t+\Delta t$ by the method of fractional time steps (due to Marchuk [15]);

$$\zeta^*_{k,l} = \zeta^n_{k,l} - \frac{\Delta t}{\Delta x}(F^n_{k+1/2,l}-F^n_{k-1/2,l})$$

and

$$\zeta^{n+1}_{k,l} = \zeta^*_{k,l} - \frac{\Delta t}{\Delta y}(G^*_{k,l+1/2}-G^*_{k,l-1/2})$$

where "*" indicates some intermediate value between t and $t+\Delta t$. The flux F^n involves ζ^n and u^n while the flux G^* involves ζ^* and v^n.

IV. Numerical Results

A number of different variations on a particular problem have been run with the modified-rigid-lid model. The basic problem is the same one that was studied in the free-surface case—a constant depth, square ocean basin is divided into 26 equally spaced zones in each direction and is subjected to a zonal wind stress. Since the curl of the wind stress does not change sign within the basin, no gulf-stream separation is anticipated. The ocean is initially at rest and the transient solution is dominated by Rossby waves [16].

We shall be concerned with two aspects of these calculations. First, we will

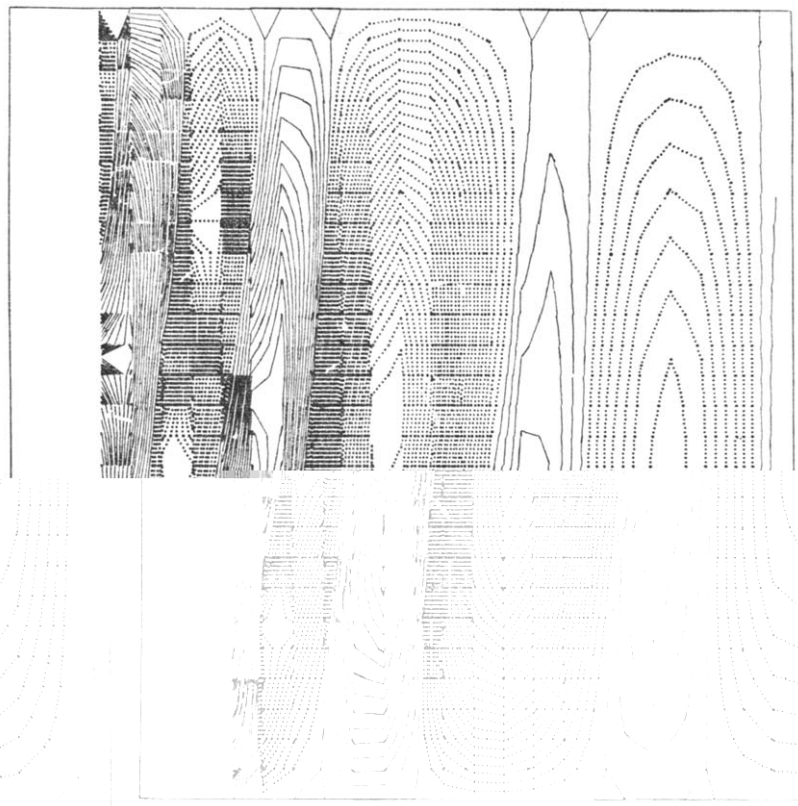

FIG. 1. Contour lines of the north–south velocity component (v) at day 29 for $\gamma^2 = 0$ (the unmodified-rigid-lid case). The plotting convention is positive (northward) or zero values of v appear as solid lines; negative values of v appear as broken lines. The contour interval is 0.0375 km/hr. The first two western zones are not plotted so that the rest of the field may be adequately defined. The same plotting convention holds through Fig. 4.

demonstrate that, with the proper choice for γ, the modified-rigid-lid solutions can be brought into approximate agreement with the free-surface solutions. We will also inquire into the dependence of the solution upon the value of the horizontal eddy viscosity coefficient.

For the investigation undertaken here it is sufficient to make qualitative rather than quantitative comparisons—to this end, contour plots of the north–south component of velocity are presented here. As before, the first two western zones are deleted from the plot so that the resolution necessary for the rest of the basin gives a tolerable picture overall. The contour interval in the v plots is 3.75×10^{-2} km hr^{-1} which, for a depth of 0.4 km compares with the contour interval 1.5×10^{-2} km^2 hr^{-1} for Hv in the free-surface case. The plotting convention is: solid lines correspond to positive or zero values of v; broken lines correspond to negative (southward) values. To give a more complete picture of the flow field, some plots of the streamfunction are also included. With these

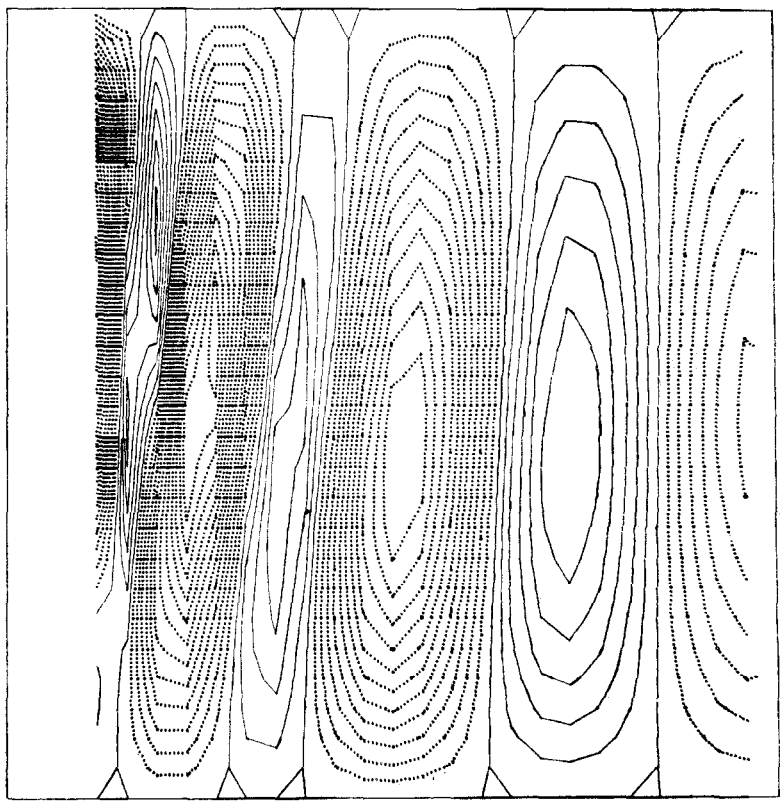

FIG. 2. Contour lines of v at day 29 for $\gamma^2 = f_0^2/gH$.

are associated a contour interval of 106 km^2 hr^{-1}. As before, these computer produced contour plots are unaided by human interpretation.

Since the evolutionary details of the transient solution were given elsewhere for this basin and windstress [1], it is not necessary to repeat them here. Rather, we will show the rigid-lid and modified-rigid-lid solutions at 29 days of model time—these may be compared with Figs. 12 and 22 from the previous article.

Unless otherwise mentioned, the parameters involved have the following values: $\Delta t = 2$ hr, $\kappa = 36$ km^2/hr (10^8 cm^2/sec), $\Delta x = 170$ km, $f_0 = 0.18$ hr^{-1}, $\beta = 0.64 \times 10^{-4}$ km^{-1} hr^{-1}, $H = 0.4$ km, $K_D = 0.004$ km^2 hr^{-2}, $Y = 4440$ km.

Figures 1 through 4 are contour plots of the north–south velocity field (v) at day 29 for the following four cases: $\gamma^2 = 0$, $gH\gamma^2 = f_0^2$, $gH\gamma^2 = (f_0 + \beta Y/2)^2$, $gH\gamma^2 = (f_0 + \beta Y)^2$. In each of these cases, $\kappa = 36$ km^2 hr^{-1}. As γ increases from

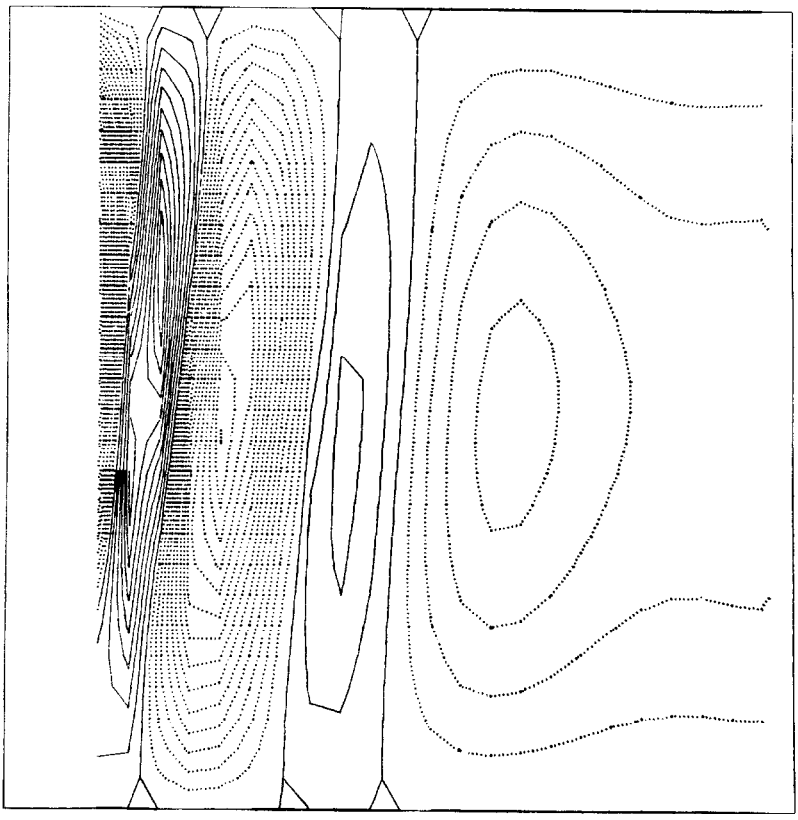

FIG. 3. Contour lines of v at day 29 for $\gamma^2 = (f_0 + \beta Y/2)^2/gH$. This figure compares favorably with Fig. 12 of Ref. [1].

zero, the phase velocity of Rossby waves decreases (Eq. II-7) and we see that as γ increases, the fixed-surface solution first becomes more like the free-surface solution, and then less like it. Figure 5 is a plot of the streamfunction at day 29 for $gH\gamma^2 = (f_0 + \beta Y/2)^2$. It compares favorably with Fig. 22 of the free-surface article. From Figs. 3 and 5 we conclude that the choice

$$\gamma^2 = (f_0 + \beta Y/2)^2/gH$$

is a reasonable one for matching free- and modified-fixed-surface solutions. That is, the best value of f to be used in Eq. II-8 is apparently the value obtained by averaging f over the basin under consideration.

In the free-surface model, it was found that a nonlinear eddy viscosity permitted small scales of motion to develop without the onset of computational instability.

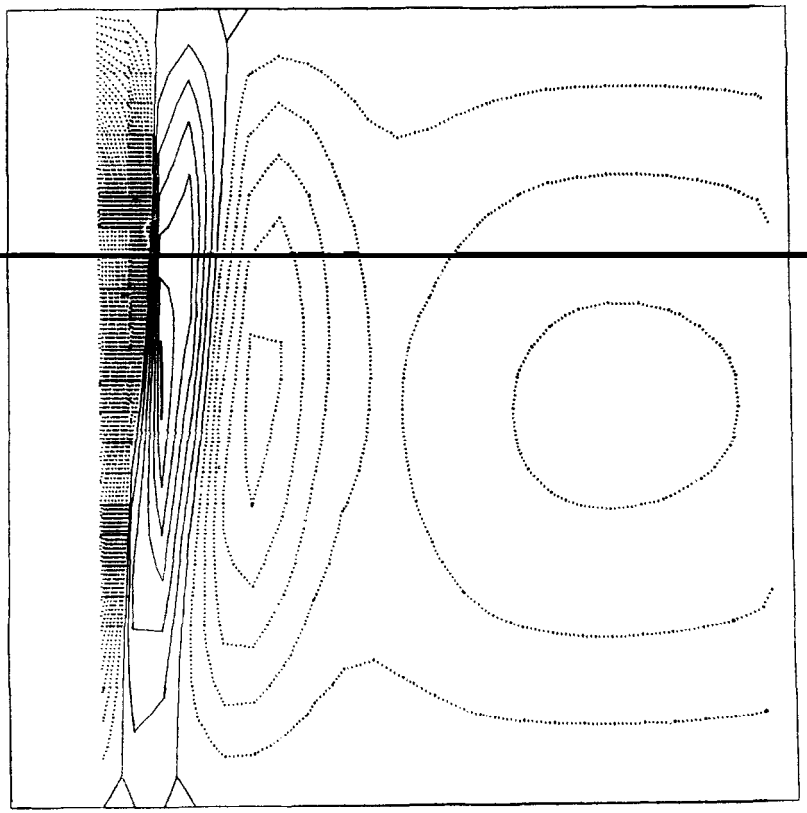

FIG. 4. Contour lines of v at day 29 for $\gamma^2 = (f_0 + \beta Y)^2/gH$. Comparison with Fig. 12 of Ref. [1] shows that the Rossby wave phase speed has been slowed too much by this choice of γ^2.

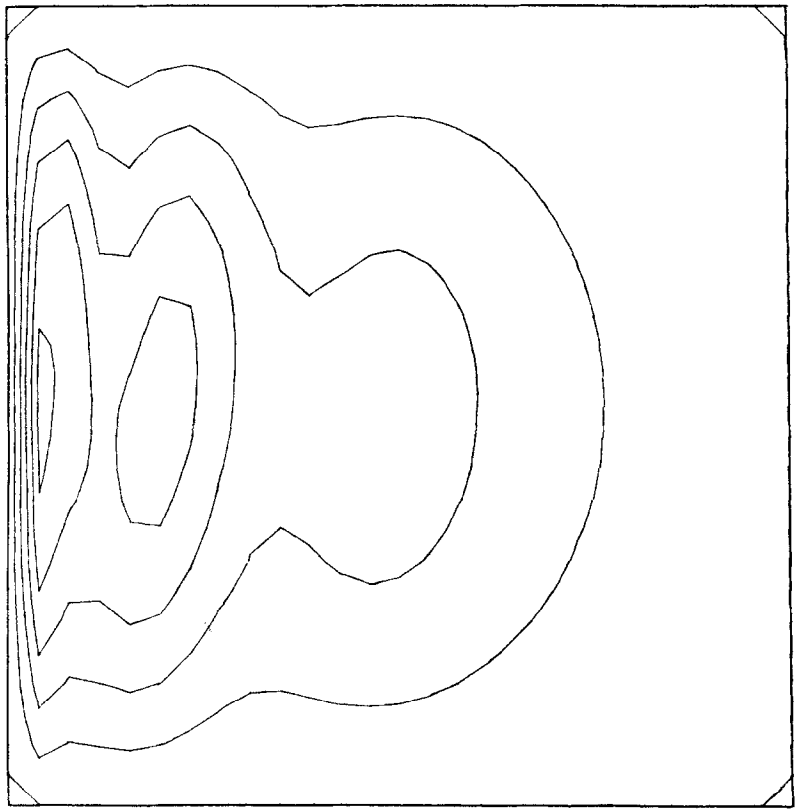

FIG. 5. The streamfunction at day 29 for $\gamma^2 = (f_0 + \beta Y/2)^2$. This compares quite well with Fig. 22 of Ref. [1]. The contour interval is 106 km^2 hr^{-1}.

Since this is permitted, not caused, by the nonlinear viscosity formulation, it would seem to follow that the same phenomena would be observed here. However, this is not the case. In fact, the fixed-surface model will operate (at least for the time scales of interest here) with no eddy viscosity at all and Fig. 6 is a contour plot of the streamfunction at day 29 for $\kappa = 0$ and $\gamma = 0$. It is seen that the large scales are quite intense relative to the viscous solution and that no small scales have developed at this time—this requires a revision of the explanation previously offered.

Fjortoft [17] considered the spectral properties of two dimensional nondivergent flows and noted that if energy initially occurs in (at least) three large scales, the nonlinear advective terms would cause it to cascade into smaller scales. However, the resulting ratio of energy in small scales to energy in large scales is less than the square of the scale lengths. The single mode, large scale forcing function

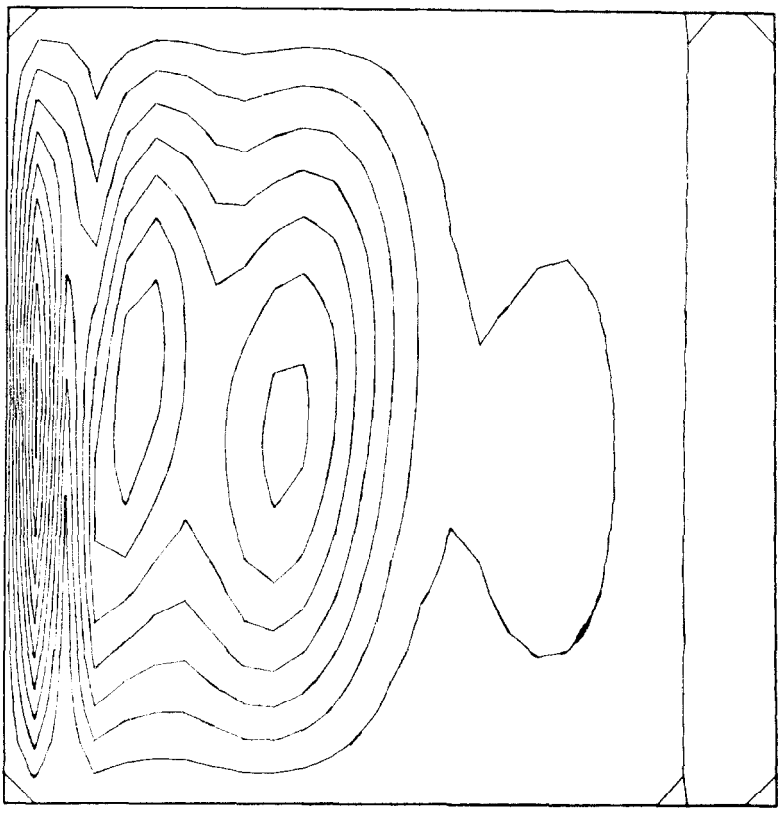

FIG. 6. The streamfunction for the inviscid case ($\kappa = 0$) at day 29 for $\gamma^2 = 0$. Comparison with Fig. 5 shows, in addition to the effect of γ, the intensification of the flow field. The gyre that appeared in the nonlinear viscosity solution (Ref. [1], Fig. 19) is absent here.

used here would then seem to preclude the importance of the nonlinear energy cascade for early times. Thus Fjortoft's analysis apparently accounts for the lack of small scale activity observed in the early transient phase of the nondivergent solution, but we must look elsewhere for an explanation for the free-surface solution.

A significant difference between free- and fixed-surface models is that both potential and kinetic energy are associated with the former while only kinetic energy may appear in the latter. Thus there is a possibility of energy exchange in free-surface models that does not occur in rigid-lid models. Since the potential-kinetic transfer term is nonlinear, it is likely that this interaction accounts for the small scale motions observed in the free-surface model.

Figure 7 is a plot of the kinetic energy for the first 25 days for five different

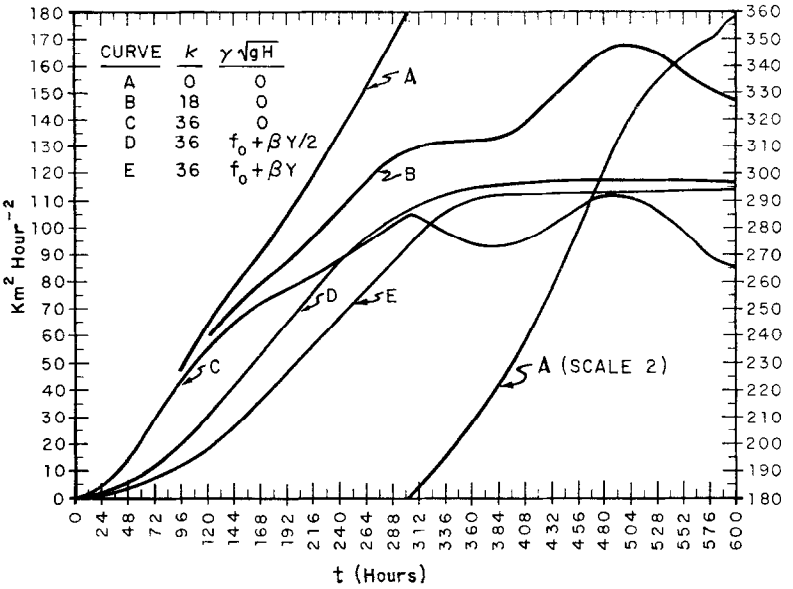

FIG. 7. The kinetic energy for the first 25 days for several problems. Curves D and E show a small amplitude oscillation in kinetic energy after the initial spin-up time, but it is not apparent on this scale

problems. There are three different eddy viscosity coefficients for the unmodified-rigid-lid case ($\gamma = 0$; $\kappa = 0, 18, 36$ km^2 hr^{-1}). For the viscous case ($\kappa = 36$) there are three different values of γ; $gH\gamma^2 = 0$, $(f_0 + \beta Y/2)^2$, and $(f_0 + \beta Y)^2$. The last two cases show a small amplitude oscillation for $t > 360$ hours.

On a CDC 6600 computer, it takes 0.0107 minutes to compute one cycle (2 model-hr) in the rigid-lid case. For the free-surface model, it takes 0.00348 min to compute one cycle (0.125 model-hr). The rigid-lid model is thus five times faster than the free-surface model. Stated another way: to obtain a barotropic solution for a certain number of model hours will take five times more computer time with the free-surface model than with the rigid-lid model. It is expected that the factor of five holds for baroclinic as well as barotropic solutions so that for large scales of motion ($\lambda \gg 340$ km), it is certainly more efficient to use the modified-rigid-lid model than the free-surface model. However, as the scales of motion become smaller, Gates [18] has shown that the effects of a free surface become more important. Thus at some point it will become necessary to use a free-surface model in order to obtain accurate transient solutions.

V. Summary

We have compared viscous numerical solutions from a modified-rigid-lid model with those obtained from a free-surface model and have found that the large scales of the two qualitatively agree if the Helmholtz parameter is chosen to be

$$\gamma^2 = (f_0 + \beta Y/2)^2/gH.$$

However, a small scale transient gyre appeared in the free-surface solutions that was absent from all (even the inviscid) solutions obtained with the modified-rigid-lid model. The nonlinear potential-kinetic energy transfer term thus appears to be more important than the energy cascade (due to nonlinear advection) in creating small scales from large at early times.

It is concluded that the relative computational efficiency of the rigid-lid model makes it adequate for integrations in which small scale motions are unimportant. This is particularly true for long term climatological integrations involving years of model time and months of computer time. However, for an accurate representation of small scale motions in transient solutions, the free-surface model is a necessity.

Acknowledgment

This work was performed under the auspices of the United States Atomic Energy Commission.

References

1. W. P. Crowley, A numerical model for viscous, free-surface, barotropic, wind-driven ocean circulations, *J. Comp. Phys.* **5** (1970), 139.
2. S. Manabe and K. Bryan, Climate calculations with a combined ocean-atmosphere model, *J. Atmos. Sci.* **26** (1969), 786.
3. P. D. Thompson, "Numerical Weather Analysis and Prediction," MacMillan, New York, 1961.
4. K. Bryan, A numerical investigation of a nonlinear model of a wind-driven ocean, *J. Atmos. Sci.* **20** (1963), 594.
5. P. Berdahl, "Oceanic Rossby Waves: A Numerical Rigid-Lid Model," University of California, Lawrence Radiation Laboratory, Livermore Report UCRL-50547, 1968.
6. B. Bolin, An improved barotropic model and some aspects of using the balance equation for three-dimensional flow, *Tellus*, **8** (1956), 61–75.
7. A. Wiin-Nielsen, On barotropic and baroclinic models, with special emphasis on ultra-long waves, *Monthly Weather Rev.* (May 1959), 171–183.
8. M. S. Longuet-Higgins, Planetary waves on a rotating sphere. II, *Proc. Roy. Soc. Ser. A* **284** (1965), 40–68.
9. R. W. Hockney, A fast direct solution of Poisson's equation using fourier analysis, *J. Ass. Comp. Mach.* **12** (1965), 95–113.

10. G. VERONIS, Wind driven ocean circulation. Part 2. Numerical solutions of the non-linear problem. *Deep Sea Res.* **13** (1966), 31–56.
11. S. K. GODUNOV AND V. S. RYABENKI, "Theory of Difference Schemes," (E. Godfredsen, Transl.), p. 146, North-Holland Publishing Co., Amsterdam, 1964.
12. R. D. RICHTMYER AND K. W. MORTON, "Difference Methods for Initial Value Problems," 2nd ed., p. 198, Interscience, New York, 1967.
13. H. W. ELLSAESSER, private communication.
14. W. P. CROWLEY, Numerical advection experiments, *Monthly Weather Rev.* **96** (1968), 1–11.
15. G. MARCHUK, Theoretical model for weather forecasting, *Dokl. Akad. SSSR* **155** (1964), 1062–1065.
16. W. L. GATES, A numerical study of transient Rossby-waves in a wind-driven homogeneous ocean, *J. Atmos. Sci.* **25** (1968), 3–22.
17. R. FJØRTOFT, On the changes in the spectral distribution of kinetic energy for two-dimensional, nondivergent flow, *Tellus* **5** (1953), 225–230.
18. W. L. GATES, On the dynamical formulation of the large-scale momentum exchange between atmosphere and ocean, *J. Marine Res.* **24** (1966), 105–112.